Spectrotemporal dynamics of a two-coupled-mode laser

E. Lacot, F. Stoeckel, D. Romanini, and A. Kachanov
Laboratoire de Spectrométrie Physique (UMR 5588), Université Joseph Fourier de Grenoble, Boîte Postale 87, 38402 Saint-Martin-d'Hères Cedex, France
(Received 21 April 1997)

In their review about intracavity laser spectroscopy, P. E. Toschek and V. Baev [in *Laser Spectroscopy and New Ideas*, edited by W. M. Yen and M. D. Levenson, Springer Series in Optical Science (Springer, Berlin, 1987)] have shown that multimode lasers are needed to obtain a high sensitivity. In this paper we show that two modes is enough. We discuss first the ideal case where only the spontaneous emission limits the sensitivity. In a second part we take into account the spatial hole burning, which couples the two modes and has for effect a lower limitation of the sensitivity. Analytical expressions are given for the modified absorption coefficient and the time evolution of the intensity of the two modes is calculated by numerical integration. [S1050-2947(98)10405-5]

PACS number(s): 42.62.Fi

I. INTRODUCTION

A broadband laser with an absorption cell inside the cavity is similar to a multipass cell with an equivalent pass length $L_{\mathrm{eq}}=ct_g$, where c is the speed of light and t_g is the ''generation time.'' This is the time difference between the moment when the gain in the cavity becomes larger than the losses and the moment when the laser spectrum is observed [1–4]. Since the introduction of the method of intracavity laser absorption spectroscopy (ICLAS) in the early 1970s (Refs. [5–7]) several theoretical and experimental studies have been concerned with the dynamics of multimode lasers. This dynamics governs ICLAS and determines up to which generation time the equivalence with a multipass cell is valid (limiting the sensitivity) [8–12] and accurate information about absorption spectra may be obtained [2–4].

In the description of an ''ideal'' intracavity spectrometer, the individual modes of a broadband laser are only coupled to the gain medium and do not interact with each other. In this case one may achieve the ultimate sensitivity of ICLAS, which is limited only due to the spontaneous emission [13,14]. The equivalent absorption path length L_{eq} grows linearly with the generation time t_g up to a characteristic time τ_{sp} where L_{eq} saturates to a stationary value. An estimation of τ_{sp} for a Ti:sapphire laser gives a value of the order of 1 s, corresponding to $L_{\mathrm{eq}}\approx 300.000$ km [8].

The behavior of a ''real'' intracavity spectrometer appears to be quite different. In particular, the time when the sensitivity stops growing is usually much less than τ_{sp}. This effect is mainly attributed to nonlinear coupling among the laser modes [15–18] that may arise in several ways [17–26]. In particular, four-wave mixing (FWM) may result from the interference of different modes in the temporal and spatial domain [24–26]. Spatial hole burning (SHB) [27–30], which can be considered as a degenerate case of FWM, is mainly responsible for nonlinear mode coupling in the case of standing-wave solid-state lasers.

Our purpose here is to show that ICLAS, which usually relies on highly multimode lasers, is also possible with a bimode laser. Then, the sensitivity limit due to nonlinear mode couplings in a multimode laser can be understood by a simple model of a two-coupled-modes laser. This model, based on rate equations including SHB [28–30], gives a good interpretation of ICLAS experimental results [8,9]. Most of the analytical and numerical results obtained for a bimode laser can be extrapolated to a highly multimode laser.

This paper is organized as follows. In Sec. II, we introduce a model for the multimode laser that takes into account the intracavity absorption, the contribution of the fluorescence in each mode, and the SHB mode coupling. In Sec. III we show that ICLAS is also possible with a bimode laser and that, in the general case [8–10], the relaxation oscillations occurring in solid-state lasers do not affect the dynamics of intracavity absorption. Then in the ideal ICLAS case, where the dynamics is only limited by the spontaneous emission, we discuss the influence of the laser parameters on the sensitivity limit. In Sec. IV, we show that a small coupling coefficient is sufficient to influence the ICLAS sensitivity as well as the accuracy of the determination of the absorption coefficient. In the case of weak and strong coupling between two modes we also give an analytical expression of the saturation time τ_{nl}, which is compared to τ_{sp} for different values of the laser parameters.

II. EQUATIONS OF MOTION

Let us consider the following set of coupled rate equations for the laser, where we take into account the spontaneous emission and the nonlinear mode coupling by SHB. Our equations are an adapted form introduced by Baer [29] and used by several other authors [30,31]:

$$\frac{d}{dt}I_i=\gamma(N_i-1)I_i+\gamma f N_i-\gamma p_i I_i,$$

$$\frac{d}{dt}N_i=N_0 g_i-N_i-N_i\sum_j C_{ij}g_j I_j, \qquad (1)$$

where I_i and N_i are, respectively, the normalized intensity and the normalized population inversion associated with the ith longitudinal mode, γ is the cavity decay rate in units of

TABLE I. Typical operating parameters.

Parameter	Dye laser	Solid-state laser
Emission cross section σ	10^{-16} cm^2	10^{-19} cm^2
Population lifetime T_1	10^{-9} s	10^{-4} s
Photon lifetime T	100 ns	100 ns
Mode volume V_c	10^{-3} cm^3	10^{-3} cm^3
Absorption coefficient α_i	10^{-7} cm	10^{-7} cm^{-1}
$\gamma = T1/T$	10^{-2}	10^{3}
$f = \sigma c T_1 / V_c$	3×10^{-12}	3×10^{-10}
$p_i = \alpha_i c T$; ($c = 3\times10^{10}$ cm/s)	3×10^{-4}	3×10^{-4}

the population inversion decay rate (we assume that the decay rate is the same for all the modes), and γp_i describes the intracavity absorption for the ith mode.

The parameter g_i is the ratio of the gain of the ith mode to that of the mode with the highest gain. The pump parameter N_0 is scaled in a way that lasing occurs for $N_0 > 1$. The effect of the spontaneous emission is described by the parameter f, which has been added to the equations for the intensity. In the set of Eq. (1) the time is a reduced time expressed in units of the population inversion lifetime (T_1). Typical operating parameters are given in Table I.

A crucial role in the dynamics of a multimode laser is played by the ratio of the cross-saturation parameter C_{ij} to the self-saturation parameter C_{ii} [32]. For SHB, the cross saturation parameter C_{ij} is a measure of the competition among the various longitudinal modes for a given population inversion. By using these rate equations we have made the usual simplifying approximation that the coefficients C_{ij} are time and pump independent [30,31].

For these approximations, the coefficients C_{ij} are then given by

$$C_{ij} = \frac{\int_{z_0-\ell/2}^{z_0+\ell/2} \sin^2 \frac{m_i \pi z}{L} \sin^2 \frac{m_j \pi z}{L}\, dz}{\int_{z_0-\ell/2}^{z_0+\ell/2} \sin^4 \frac{m_i \pi z}{L}\, dz},$$

where m_i is the number of half-wavelengths of the ith mode. The integration is over the length ℓ of the active medium, whose center is located at a distance z_0 from one of the two cavity mirrors (Fig. 1).

When the length of the gain medium is much larger than the wavelength one obtains, in the usual case,

$$C_{ij} = \tfrac{2}{3} + \tfrac{1}{3}\ \mathrm{sinc}\left(\frac{\pi \ell}{L}(m_i - m_j)\right) \times \cos\left(2\pi \frac{z_0}{L}(m_i - m_j)\right)$$

with

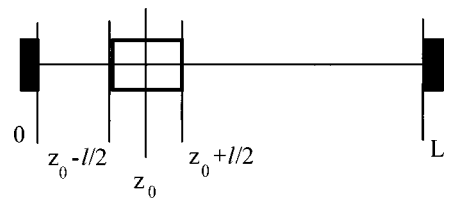

FIG. 1. Schematic of the standing-wave cavity laser.

$$C_{ii} = 1 \quad \text{and} \quad C_{ij} = C_{ji}.$$

By introducing the coupling coefficient $K_{ij} = 1 - C_{ij}$, Eq. (1) may be rewritten:

$$\frac{d}{dt} I_i = \gamma(N_i - 1) I_i + \gamma f N_i - \gamma p_i I_i,$$

$$\frac{d}{dt} N_i = N_0 g_i - N_i - N_i \sum_j g_j I_j + N_i \sum_{j \neq i} K_{ij} g_j I_j. \qquad (2)$$

In the case of small coupling ($K_{ij} \ll g_j$) and using the adiabatic approximation ($\gamma \ll 1$) the set of Eq. (2) can be written as

$$\frac{d}{dt} I_i = -\gamma I_i - \gamma p_i I_i + \frac{\gamma N_0 g_i}{1 + \Sigma_j g_j I_j}(I_i + f\,) + \frac{\gamma N_0 g_i}{(1 + \Sigma_j g_j I_j)^2} I_i \sum_{j \neq i} K_{ij} g_j I_j. \qquad (3)$$

This equation describes the dynamics of a multimode laser in the case when the lifetime of the photons in the cavity is much larger than the lifetime of the population inversion. The last term describes the effect of the small mode coupling due to the SHB.

III. IDEAL ICLAS (NO MODE COUPLING)

A. Linear absorption

In the ideal intracavity spectrometer description ($K_{ij} = 0$) all the modes interact only with the (same) population inversion. If we neglect the spontaneous emission ($f = 0$), Eq. (2) can be analytically solved in the adiabatic case ($\gamma \ll 1$). For a bimode laser with $g_1 = 1$, $g_2 < 1$, $p_1 = 0$, and $p_2 \neq 0$, we obtain

$$I_1(t) = \frac{I_1(0) I_{\mathrm{tot}}}{I_1(0) + I_2(0) \exp[-\gamma(1 - \hat{g}_2)t]},$$

$$I_2(t) = \frac{I_2(0) I_{\mathrm{tot}} \exp[-\gamma(1 - \hat{g}_2)t]}{I_1(0) + I_2(0) \exp[-\gamma(1 - \hat{g}_2)t]}, \qquad (4)$$

where $I_{\mathrm{tot}} = I_1(t) + I_2(t) = N_0 - 1$, and $\hat{g}_1 = g_1$, $\hat{g}_2 = g_2 - p_2$ are the difference between gain and loss of the ith mode. By taking the ratio between the two previous equations, we obtain the following simple relation:

$$\frac{I_2(t)}{I_1(t)} = \frac{I_2(0)}{I_1(0)} \exp[-\gamma(1 - \hat{g}_2)t]. \qquad (5)$$

Equation (5) is the analogue to the Beer-Lambert law with an absorption coefficient $\alpha = \gamma(1 - \hat{g}_2)/c$ and an equivalent absorption path length $L_{\mathrm{eq}} = ct$, where t is the running time of the laser. This time is also called generation time in the ICLAS dynamics.

In a logarithmic scale the time evolution of $I_2(t)/I_1(t)$ is a perfect straight line with a slope given by

$$\frac{d}{dt} \ln\left(\frac{I_2(t)}{I_1(t)}\right) = -\gamma(1 - \hat{g}_2). \qquad (6)$$

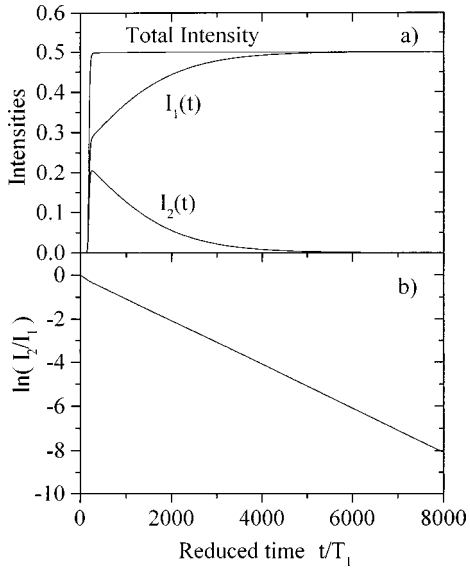

FIG. 2. Numerical simulation of the dynamical behavior of a bimode dye laser. (a) Intensities I_1, I_2 and of the total intensity I_{tot}, (b) $\ln(I_2/I_1)$ for the following parameters: $\gamma=2\times10^{-1}$, $\hat{g}_1=1$, $\hat{g}_2=0.995$, $N_0=1.5$, $f=0$, $K_{ii}=0$, $K_{ij}=0$, and $i=1,2$.

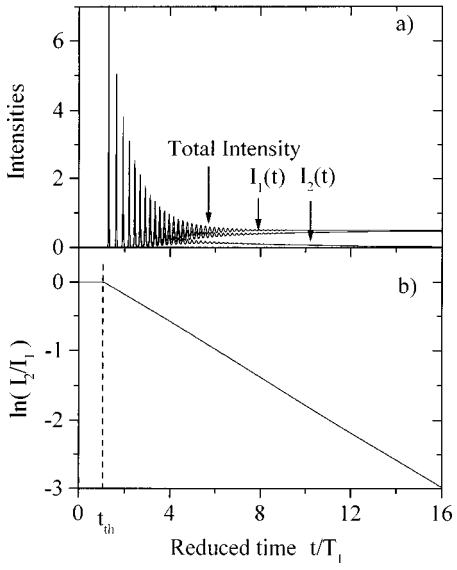

FIG. 3. Numerical simulation of the dynamical behavior of a bimode solid-state laser. (a) Intensities I_1, I_2 and of the total intensity I_{tot}, (b) $\ln(I_2/I_1)$ for the following parameters: $\gamma=2\times10^3$, $\hat{g}_1=1$, $\hat{g}_2=0.9999$, $N_0=1.5$, $f=0$, $K_{ii}=0$, $K_{ij}=0$, and $i=1,2$. The time t_{th} is the time needed by the population inversion to reach the threshold.

We have numerically solved, using a Runge-Kutta method with variable integration step, the exact dynamics given by the coupled set of equations (2) for a bimode laser. For $\gamma \ll 1$ (i.e., dye lasers) and for the following values of the parameters:

$$K_{ij}=0, \quad f=0,$$

$$\gamma=2\times10^{-1}, \quad \hat{g}_1=1, \quad \hat{g}_2=0.995, \quad N_0=1.5,$$

Figure 2 shows the time evolution of the two modes $[I_1(t)$ and $I_2(t)]$ and of the total intensity $[I_1(t)+I_2(t)]$. After a relatively quick turn on, we see that the total intensity remains constant [Fig. 1(a)]. The intensity $I_2(t)$ of the mode having the lowest gain decreases exponentially in time, while the intensity $I_1(t)$ of the other mode reaches a stationary state. During this period of intensity redistribution, the logarithm of the ratio of the intensities of the two modes follows the predicted Beer-Lambert law [Fig. 2(b)] with a slope given by Eq. (6).

When $\gamma \gg 1$ (i.e., solid-state lasers), the adiabatic elimination of the population inversion is no longer possible and the analytical expression of Eq. (4) is no longer valid. Figure 3(a) shows that the dynamical behavior of $I_1(t)$, $I_2(t)$, and $I_{\text{tot}}(t)$ exhibits relaxation oscillations. Despite this complex temporal behavior, the logarithm of the ratio of $I_2(t)$ and $I_1(t)$ is still a straight line after an initial delay (Fig. 3b). The ratio $I_2(t)/I_1(t)$ follows the same Beer-Lambert law if we replace the time t in Eq. (5) by $t-t_{\text{th}}$. By plotting the time evolution of the population inversion it can be shown that this time delay t_{th} is the time needed for the population inversion to reach lasing threshold. As was also found for a multimode laser [8], t_{th} decreases when N_0 increases.

In conclusion, a bimode laser with negligible spontaneous emission and without any mode coupling, follows the same dynamics as a highly multimode laser (dye or solid-state lasers).

B. Sensitivity limit

Let us now estimate the influence of the spontaneous emission ($f\neq0$) on a bimode laser. We can estimate this influence by expressing the stationary solutions of Eq. (2) as

$$I_1^{\text{st}}=\frac{2(N_0-1)f}{2f-(1-\hat{g}_2)(N_0-1)+\sqrt{(1-\hat{g}_2)^2(N_0-1)+4f^2}},$$

$$I_2^{\text{st}}=\frac{2(N_0-1)f}{2f+(1-\hat{g}_2)(N_0-1)+\sqrt{(1-\hat{g}_2)^2(N_0-1)+4f^2}}. \tag{7}$$

I_2^{st} no longer goes to zero since at long generation times the spontaneous emission stops both the time evolution of $I_1(t)$ and of $I_2(t)$. For $1-\hat{g}_2 \gg f$ (typical operating condition), we obtain

$$I_1^{\text{st}}=(N_0-1), \quad I_2^{\text{st}}=\frac{f\hat{g}_2}{(1-\hat{g}_2)}. \tag{8}$$

Figure 4 shows the effect of the spontaneous emission for different values of the pump parameter N_0. The time evolution of $\ln[I_2(t)/I_1(t)]$ is obtained by numerically solving the set of Eq. (2).

We can see that, as in the case with no spontaneous emission, the relaxation oscillations of the intensities of the two modes $I_1(t)$ and $I_2(t)$ disappear in their ratio. This figure also shows that, for short times, the ratio $I_2(t)/I_1(t)$ follows a Beer-Lambert law with a decay constant equal again to $-\gamma(1-\hat{g}_2)$. After a characteristic time τ_{sp}, the spontaneous emission stop the laser dynamics and the intensities of the modes reach stationary values.

As we can see in Fig. 4 the saturation time τ_{sp} is defined by the intersection point between the straight line of slope

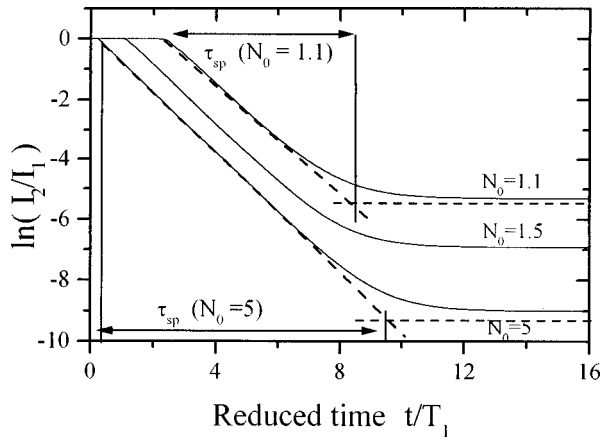

FIG. 4. Numerical simulation of the time evolution of $\ln(I_2/I_1)$ for different values of the pump parameter N_0 for the following parameters: $\gamma=5\times10^3$, $\hat{g}_1=1$, $\hat{g}_2=0.9998$, $f=10^{-7}$, $K_{ii}=0$, $K_{ij}=0$, and $i=1,2$. In each case the slope of the Beer-Lambert law is given by $\gamma(1-\hat{g}_2)$ and the saturation time $\tau_{\rm sp}$ due to spontaneous emission increases with N_0.

$-\gamma(1-\hat{g}_2)$ (Beer-Lambert law) and the horizontal line given by $\ln(I_2^{\rm st}/I_1^{\rm st})$ (steady-state value due to spontaneous emission). Using Eq. (8), $\tau_{\rm sp}$ is given by

$$\tau_{\rm sp}\approx\frac{1}{\gamma(1-\hat{g}_2)}\ln\left(\frac{(N_0-1)(1-\hat{g}_2)}{f\hat{g}_2}\right). \tag{9}$$

Equation (9) predicts, in agreement with the numerical results shown in Fig. 4, an increase of the maximum equivalent path length $L_{\rm eq}=c\tau_{\rm sp}$ with the pump power excess above the threshold (N_0-1). One could therefore expect to increase the ICLAS sensitivity limit by increasing the pumping level. Most experiments, however, show just the opposite dependence [15], which means that the temporal dynamics of real lasers is dominated by mode coupling rather than by spontaneous emission.

IV. REAL ICLAS (WITH MODE COUPLING)

While in the previous paragraph we have neglected all interaction among the laser modes, here we show that this interaction can play an important role in the limitation of the sensitivity of a bimode ICLAS spectrometer. We will assume that SHB is the only interaction phenomenon among the modes.

A. Nonlinear absorption

In condition $(K_{ij}\neq0)$, from the last term of Eq. (3), we can see that nonlinear mode coupling due to the SHB will significantly modify the dynamics of the ith mode only for sufficiently long generation times:

$$t>\tau_m=\frac{\langle I_i\rangle}{F_{\rm nl}}, \tag{10}$$

where the variable within brackets is averaged in time and with the nonlinear force $F_{\rm nl}$ given by

$$F_{\rm nl}=\left\langle\frac{\gamma N_0 g_i}{(1+\Sigma_j g_j I_j)^2}\,I_i\sum_{j\neq i}K_{ij}g_j I_j\right\rangle.$$

For a bimode laser, with $g_i\approx1$ and $\sum_j g_j I_j\approx N_0-1$,

$$\tau_m=\frac{N_0}{\gamma\langle I_1\rangle K}\approx\frac{2N_0}{\gamma(N_0-1)K}. \tag{11}$$

Thus, for a given generation time the effects of the SHB coupling that are negligible near the threshold $(N_0\approx1)$ increase with the pump power.

For intracavity spectroscopy, the first effect of nonlinear mode coupling is a modification of the measured absorption coefficient. Indeed, if we neglect spontaneous emission $(f=0)$, Eq. (3) shows that before saturation

$$\frac{d}{dt}\ln\left(\frac{I_2(t)}{I_1(t)}\right)=-\gamma(1-\hat{g}_2)+\frac{\gamma K\hat{g}_2}{N_0}\,[I_1(t)-I_2(t)]. \tag{12}$$

This expression has to be compared with Eq. (5). We have now a nonlinear absorption law with a modified absorption coefficient that depends on the coupling coefficient K, the pump power parameter N_0, and the mode intensity I_i.

For a short generation time $(t\ll\tau_m)$, $I_1(t)$ is of the same order of magnitude than $I_2(t)$. As a result the slope of the curve is given by $-\gamma(1-\hat{g}_2)$ and the absorption coefficient of the absorption law is approximately equal to $\alpha=\gamma(1-\hat{g}_2)/c$ as in the ideal ICLAS case.

For a longer generation time $(t\approx\tau_m)$, I_1 becomes higher than I_2 and the modified absorption coefficient α_m is dependent on the pump power parameter N_0. By taking $I_1\approx N_0-1$, we obtain

$$\alpha_m=\frac{\gamma(1-\hat{g}_2)}{c}-\frac{\gamma K\hat{g}_2}{c}\,\frac{(N_0-1)}{N_0}. \tag{13}$$

Figure 5 shows the time evolution of $\ln(I_2/I_1)$ obtained by numerical solution of the set of Eq. (2) for $K_{ij}\neq0$ and for different values of the pump parameter N_0.

In agreement with Eqs. (10) and (11), one can see that at short generation time the effects of nonlinear mode coupling are negligible and, for all the pump parameter, $I_2(t)/I_1(t)$ follows a Beer-Lambert law with a decay constant equal to $-\gamma(1-\hat{g}_2)$.

For longer generation time, Fig. 5 also shows that the effect of the SHB coupling, which is negligible near the threshold $(N_0\approx1)$, increases with the pump power.

B. Nonlinear sensitivity limit

At long generation time the combined effects of nonlinear mode coupling and of spontaneous emission stop the time evolution of $I_1(t)$ and $I_2(t)$. For a bimode laser with $K_{12}=K_{21}=K$, a linear stability analysis of Eq. (2) shows that there are two types of stationary solutions, one corresponding to a weak SHB coupling, and the other to a stronger SHB coupling [32].

For a weak SHB coupling $(0\leqslant K<1-\hat{g}_2\ll\hat{g}_2)$, the stationary solution for the pump condition $N_0>1$ gives

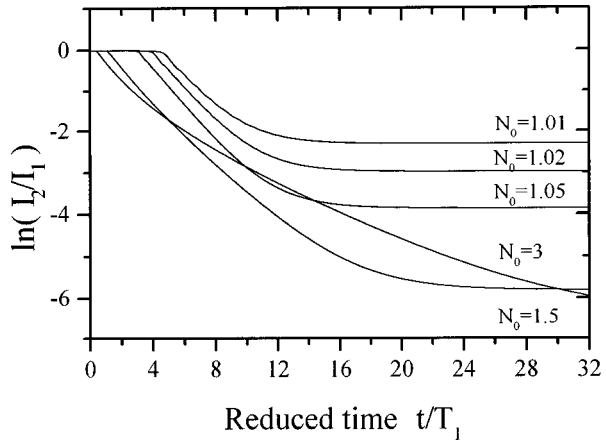

FIG. 5. Numerical simulation of the time evolution of $\ln(I_2/I_1)$ for a weak SHB coupling and for different values of the pump parameter N_0 with the following parameters: $\gamma=5\times10^3$, $\hat{g}_1=1$, $\hat{g}_2=0.9999$, $f=10^{-7}$, $K_{11}=0$, and $K_{12}=10^{-4}$.

$$I_1^{\mathrm{st}}+(N_0-1), \quad I_2^{\mathrm{st}}=\frac{fN_0\hat{g}_2}{N_0(1-K-\hat{g}_2)+K}\approx 0. \qquad (14)$$

In this case the bimode laser is again nearly single mode as in the no coupling case, but the intensity of the weakest mode is slightly modified by the SHB.

For a strong SHB coupling $(1-\hat{g}_2<K\ll\hat{g}_2)$, and for the pump condition $1<N_0<N_{\mathrm{nl}}=K/[K-(1-\hat{g}_2)]$, the stationary solution is also given by Eq. (14).

For $N_0>N_{\mathrm{nl}}$ a bimode solution exists with

$$I_1^{\mathrm{st}}=\frac{1}{K(2-K)}\,[N_0(\hat{g}_2K+1-\hat{g}_2)-K],$$

$$I_2^{\mathrm{st}}=\frac{1}{K(2-K)}\,\frac{1}{\hat{g}_2}\,\{N_0[K-(1-\hat{g}_2)]-K\}. \qquad (15)$$

Figures 5 and 6 show the time evolution of $\ln(I_2/I_1)$ for, respectively, weak and strong SHB coupling. In both case we define the saturation time τ_{nl} as the intersection point between the straight line of slope $-\gamma(1-\hat{g}_2)$ (Beer-Lambert

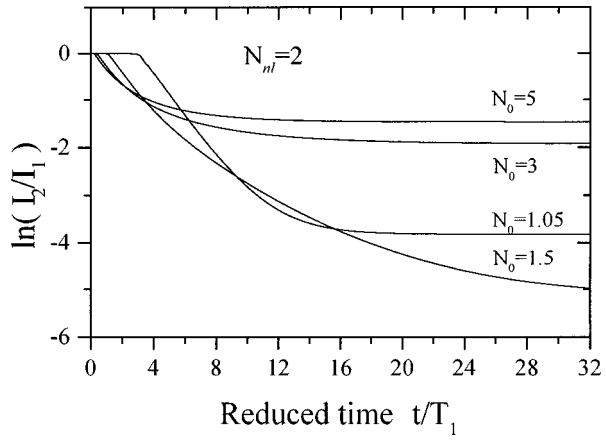

FIG. 6. Numerical simulation of the time evolution of $\ln(I_2/I_1)$ for a strong SHB coupling and for different values of the pump parameter N_0 with the following parameters: $\gamma=5\times10^3$, $\hat{g}_1=1$, $\hat{g}_2=0.9999$, $f=10^{-7}$, $K_{11}=0$, $K_{12}=2\times10^{-4}$.

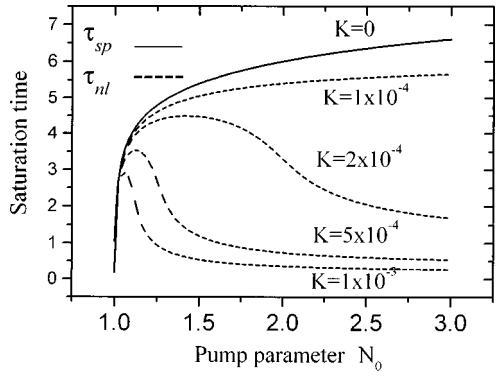

FIG. 7. Calculated values of the saturation times τ_{sp} (due to spontaneous emission) and τ_{nl} (due to nonlinear mode coupling) versus the pump parameter N_0 for different value of the coupling coefficient K and with the following parameters: $\gamma=5\times10^3$, $\hat{g}_1=1$, $\hat{g}_2=0.9999$, and $f=10^{-7}$.

law) and the horizontal line given by $\ln(I_2^{\mathrm{st}}/I_1^{\mathrm{st}})$ (steady-state value with nonlinear mode coupling). Using Eqs. (14) or (15), τ_{nl} is obtained by,

$$\tau_{\mathrm{nl}}\approx\frac{1}{\gamma(1-\hat{g}_2)}\ln\left(\frac{I_1^{\mathrm{st}}}{I_2^{\mathrm{st}}}\right). \qquad (16)$$

For weak SHB coupling (Fig. 5), the saturation behavior of the bimode laser is approximately the same as that obtained in the no coupling case (Fig. 4). The ratio of $I_2^{\mathrm{st}}/I_1^{\mathrm{st}}$ always decrease with the pump power and Eq. (16) predicts, in agreement with the numerical results, an increase of the maximum equivalent path length $L_{\mathrm{eq}}=c\tau_{\mathrm{nl}}$. Nevertheless, the saturation time τ_{nl} is always a bit smaller than τ_{sp}.

For a strong SHB coupling, Fig. 6 shows the time evolution of $\ln(I_2/I_1)$ obtained numerically from the set of Eq. (2). In this case, the saturation behavior of the bimode laser is really different. Indeed for a small value of the pump power $(N_0<\sqrt{N_{\mathrm{nl}}})$ the maximum equivalent path length $L_{\mathrm{eq}}=c\tau_{\mathrm{nl}}$ increase with pump power while for $N_0>\sqrt{N_{\mathrm{nl}}}$, $L_{\mathrm{eq}}=c\tau_{\mathrm{nl}}$ decreases with pump power. Figure 6 also show that for $N_0<N_{\mathrm{nl}}$ and before the saturation, we observe the same type of behavior as for weak SHB, but with a stronger modification of the slope and then of absorption coefficient α_m, while for $N_0>N_{\mathrm{nl}}$ I_1^{st} is of the same magnitude as I_2^{st}. As a result, the saturation of the absorption occurs rapidly.

Figure 7 shows the calculated value of τ_{sp} from Eq. (9) and τ_{nl} from Eq. (14) versus the pump parameter N_0, for different values of the coupling coefficient K. To allow direct and quantitative comparisons with the simulation results, the behaviors of saturation times τ_{sp} and τ_{nl} are studied within the same range of parameters as those used in Figs. 4–6. We observe that near the threshold of the laser, the ICLAS sensitivity is limited by spontaneous emission and the maximum equivalent path length is given by $L_{\mathrm{eq}}^{\max}=c\tau_{\mathrm{sp}}$, which increases with the pump power, while higher above the threshold, the sensitivity is governed by the mode coupling and $L_{\mathrm{eq}}^{\max}=c\tau_{\mathrm{nl}}<c\tau_{\mathrm{sp}}$, which decreases with the pump power. This is also what can be observed experimentally in multimode lasers.

C. Case of a highly multimode laser

Most of the analytical and numerical results obtained in this section can be extrapolated to a higher number of modes. For example, for a highly multimode laser, we obtain from Eq. (3)

$$\frac{I_{q_i}(t)}{I_{q_i}(0)}=\exp\left[-\gamma\left(\frac{q_i-q_0}{Q}\right)^2\left(1+\frac{\Sigma_{j\neq i}K_{qi,qj}g_{q_j}I_{q_j}}{N_0}\right)t\right]$$
$$\times\exp\left[-\gamma\left(p_{q_j}-\frac{\Sigma_{j\neq i}K_{qi,qj}g_{q_j}I_{q_j}}{N_0}\right)t\right], \qquad (17)$$

where K_{q_i,q_j} is a small coupling coefficient between the modes q_i and q_j and where we have approximated the gain distribution g_{q_j} by a Lorentzian profile with a half-width Q:

$$g_{q_i}=\frac{1}{1+\frac{(q_i-q_0)^2}{Q^2}}\approx 1-\frac{(q_i-q_0)^2}{Q^2}.$$

The first part of Eq. (17) described the time evolution of the Gaussian baseline of the laser spectrum, while the second part describes the time evolution of intracavity absorption. Equation (17) shows that the width of this baseline (or the envelope) no longer follows the well-know square-root law versus the generation time found for the multimode ideal ICLAS model [1].

In a laser just above the threshold ($I_{q0}\gg I_{q_j}$) with a cavity length satisfying the condition $L/\mathscr{l}\gg Q$, the coupling coefficient can be considered constant, $K_{q_i,q_j}\approx K$, and Eq. (17) can be rewrite as

$$\frac{I_{q_i}(t)}{I_{q_i}(0)}=\exp\left\{-\gamma\left(\frac{q_i-q_0}{Q}\right)^2\left[1+K\left(\frac{N_0-1}{N_0}\right)\right]t\right\}$$
$$\times\exp\left\{-\gamma\left[p_{q_i}-K\left(\frac{N_0-1}{N_0}\right)\right]t\right\}. \qquad (18)$$

In this equation, we have considered only the small coupling coefficient between the q_i mode and the central mode labeled q_0, which is the only one above the threshold ($I_{q0}\gg I_{qj}$). In this way, all modes interact with the central mode ($I_{q0}*I_{qj}\neq 0$) and not with their next neighbors ($I_{qi}*I_{qj}\approx 0$).

Thus, in a multimode laser, nonlinear mode coupling modifies the time evolution of the absorption line as well as the base line of the laser spectrum. As in a bimode laser, the modifications that are negligible near the threshold ($N_0\approx 1$) increase with pump power.

V. CONCLUSION

In the context of intracavity laser absorption spectroscopy (ICLAS), we have studied the spectrotemporal dynamics of a bimode laser. We have analyzed both the effect of the spontaneous emission and of the mode coupling due to SHB. In the ideal ICLAS case, where no coupling exists, a bimode laser follows the same spectro temporal dynamics as a highly multimode laser of the same kind. In this case, the sensitivity limit is determined by the contribution of the spontaneous emission and the maximum equivalent absorption pathlength $L_{\rm eq}=c\tau_{\rm sp}$ increases with the pump power.

In the real ICLAS case, nonlinear mode coupling affects the laser dynamics and the maximum equivalent path length $L_{\rm eq}=c\tau_{\rm nl}$ decreases with the pump power. The absorption coefficient determined from the time evolution of the intensities of the two modes is found to be reduced by the SHB coupling as a function of the pump power. An analytical expression of the absorption coefficient is given. By comparing $\tau_{\rm sp}$ and $\tau_{\rm nl}$, the main experimental results of a broadband intracavity spectrometer can be clearly understood. Near the threshold, the sensitivity saturation is given by the spontaneous emission, and increases with the pump power. Higher above the threshold, the sensitivity is governed by the mode coupling and the sensitivity decreases with the pump power. This is what can be observed experimentally with multimode lasers.

In this paper we have shown that intracavity spectroscopy, usually performed with a highly multimode laser, is possible with two or a few modes, in agreement with experimental results [33,34]. Finally, we have extended this two-mode model to a highly multimode laser for which we have given an analytical expression of the spectrotemporal evolution taking into account the SHB coupling between the modes.

[1] V. M. Baev, I. P. Belikova, E. A. Sviridenkov, and A. F. Suchkov, Zh. Eksp. Teor. Fiz. **74**, 43 (1978) [Sov. Phys. JETP **47**, 21 (1978)].

[2] F. Stoeckel, M. A. Melieres, and M. Chenevier, J. Chem. Phys. **76**, 2192 (1982).

[3] M. Chenevier, M. A. Melieres, and F. Stoeckel, Opt. Commun. **45**, 386 (1983).

[4] A. Campargue, F. Stoeckel, and M. Chenevier, Spectrochim. Acta Rev. **13**, 69 (1990).

[5] L. A. Pakhomycheva, E. A. Sviridenkov, A. F. Suchkov, L. V. Titova, and S. S. Churilov, Pisma Zh. Eksp. Teor. Fiz. **12**, 60 (1970) [JETP Lett. **12**, 43 (1970)].

[6] M. C. Peterson, M. J. Kurilo, W. Braun, A. M. Bass, and R. A. Keller, J. Opt. Soc. Am. A **61**, 746 (1971).

[7] T. W. Hansch, A. L. Schawlow, and P. E. Toschek, IEEE J. Quantum Electron. **8**, 802 (1972).

[8] A. A. Kachanov, A. Charvat, and F. Stoeckel, J. Opt. Soc. Am. B **11**, 2412 (1994).

[9] A. A. Kachanov, A. Charvat, and F. Stoeckel, J. Opt. Soc. Am. B **12**, 970 (1995).

[10] D. Romanini, A. A. Kachanov, E. Lacot, and F. Stoeckel, Phys. Rev. A **54**, 920 (1996).

[11] J. Sierks, V. M. Baev, and P. E. Toschek, Opt. Commun. **96**, 436 (1993).

[12] A. A. Kachanov, V. R. Mironenko, and I. K. Pashkovich, Sov. J. Quantum Electron. **19**, 95 (1989).

[13] V. R. Mironenko and V. I. Yudson, Opt. Commun. **34**, 397 (1980).

[14] S. A. Kovalenko, Sov. J. Quantum Electron. **11**, 759 (1981).
[15] E. N. Antonov, A. A. Kachanov, V. R. Mironenko, and T. V. Plakhotnik, Opt. Commun. **46**, 126 (1983).
[16] H. Atmanspacher, H. Sheingraber, and C. R. Vidal, Phys. Rev. A **33**, 1052 (1986).
[17] H. Atmanspacher, H. Sheingraber, and V. M. Baev, Phys. Rev. A **35**, 142 (1987).
[18] S. A. Kovalenko, S. P. Semin, and D. D. Toptygin, Sov. J. Quantum Electron. **21**, 407 (1991).
[19] S. A. Kovalenko and S. P. Semin, Opt. Commun. **71**, 189 (1989).
[20] A. Fleck and R. E. Kidder, J. Appl. Phys. **35**, 2825 (1964).
[21] N. G. Basov, V. N. Morozov, and A. N. Oraevskii, Zh. Eksp. Teor. Fiz. **49**, 895 (1965) [Sov. Phys. JETP **22**, 622 (1966)].
[22] L. A. Ostrovskii, Zh. Eksp. Teor. Fiz **48**, 1087 (1965) [Sov. Phys. JETP **21**, 727 (1965)].
[23] W. Jingyi and P. Mandel, Phys. Rev. A **48**, 671 (1993).
[24] I. Mc Mackin, C. Radzewicz, M. Beck, and M. G. Raymer, Phys. Rev. A **38**, 820 (1988).
[25] M. G. Raymer, Z. Deny, and M. Beck, J. Opt. Soc. Am. B **5**, 1588 (1988).
[26] V. M. Baev, J. Eschner, J. Sierks, A. Weiler, and P. E. Toschek, Opt. Commun. **94**, 436 (1992).
[27] K. Otsuka, M. Georgiou, and P. Mandel, Jpn. J. Appl. Phys., Part 2 **31**, L1250 (1992).
[28] C. L. Tang, H. Statz, and G. de Mars, J. Appl. Phys. **34**, 2289 (1963).
[29] T. Baer, J. Opt. Soc. Am. B **3**, 1175 (1986).
[30] E. Lacot and F. Stoeckel, J. Opt. Soc. Am. **9**, 2034 (1996).
[31] C. Bracikowski and R. Roy, Phys. Rev. A **43**, 6455 (1991).
[32] A. E. Siegmann, *Lasers*, (University Science, Mill Valley, California, 1986).
[33] A. Kachanov, F. Stoeckel, J. O'Brien, and A. Charvat, Appl. Opt. (to be published).
[34] V. M. Baev, J. Eschner, E. Paeth, R. Shuler, and P. E. Toschek, Appl. Phys. B: Photophys. Laser Chem. **55**, 463 (1992).